3rd US-European Competition and Workshop on Micro Air Vehicle Systems (MAV07) & European Micro Air Vehicle Conference and Flight Competition (EMAV2007), 17-21 September 2007, Toulouse, France

Unsteady Mechanical Aspects of Flexible Wings: an Experimental Investigation of Biologically Inspired MAVs

Roberto Albertani[*]
Research and Education Engineering Facility, University of Florida, Shalimar, FL, 32579

and

Bret Stanford[†], Michael Sytsma[‡], Peter Ifju[§]
Department of Mechanical and Aerospace Engineering, University of Florida, Gainesville, FL, 32611

The work presented in this paper undertakes a series of experiments to evaluate the basic structural dynamics parameters of membrane micro air vehicle (MAV) wings. These experiments determine the mode shapes, natural frequencies, and modal damping factors in ambient air, thus including viscous damping effects. Bench vibrations tests (dry tests) and naturally induced vibrations measurements in a wind tunnel are performed on 15 cm wings with different levels of membrane pre-tension, to ascertain the correlation between the reference strain energy and the modal characteristics. Non-contact measurements (using a laser Doppler vibrometer and a visual image correlation system) and base excitation techniques with an electromagnetic shaker are used. The natural frequencies and damping ratios for the elastic membrane are well defined only in the high and low pre-tension cases; the first three frequencies increase with pre-tension while the damping ratio decreases with both pre-tension and mode number. Wind tunnel tests reveal the presence of an energy spike in the wing displacement power spectra at moderate angles of attack, but only for the cases of low and no membrane pre-tension. The spike is not a structural vibration mode, and is possibly induced by vortex shedding or laminar separation bubble dynamics.

Nomenclature

α	=	angle of attack
c,b	=	wing root chord and span
C_L	=	coefficient of lift
ε_{xx} ε_{yy} ε_{xy}	=	plane strains
N	=	number of samples
S_x	=	standard deviation
$t_{v,95}$	=	uncertainty weighting factor for 95% confidence
u v w	=	Cartesian coordinate displacements
u_x	=	uncertainty interval
x y z	=	Cartesian coordinate directions

I. Introduction

STRUCTURAL flexibility is a key feature of the micro air vehicle wings developed at the University of Florida. The basic configuration of these wings is a composite laminate skeleton affixed to a membrane sheet, which is typically composed of thin latex rubber (as depicted in Figure 1) or polyester kite material. The flight performance of flexible MAVs has indicated several desirable properties directly attributable to the elastic

[*] Research Assistant Professor, REEF, University of Florida, Shalimar, FL, 32579.
[†] Research Assistant, MAE, University of Florida, Gainesville, FL, 32611.
[‡] Research Assistant, MAE, University of Florida, Gainesville, FL, 32611.
[§] Professor, MAE, University of Florida, Gainesville, FL, 32611.

nature of the wing: primarily, passive shape adaptation. Such adaptation also introduces a higher level of uncertainties in the structural dynamics.

This paper proposes several experimental techniques to evaluate the basic parameters of MAV wing structures by determining mode shapes (eigenfunctions), natural frequencies and modal damping factors. Of particular interest to the current work is the vibration of pre-stressed membrane fixed wings, a truly biologically inspired feature. For example, locusts develop specific dome-shaped sensory organs within the structure of their wings[1]. These feedback sensors respond to wing deformation in order to trigger the wing structure to operate at resonant frequencies. Furthermore, bats can control their wing characteristics by changing the level of tension in their membrane wings, thus effectively changing the wing camber and the passive aeroelastic dynamic feedback of the membrane to the aerodynamic loading[2]. The aerodynamic models and flight control design of fixed[3] and flapping wings[4] must include the wing flexibility and structural dynamics, an area where very little experimental data is available.

Figure 1. Micro air vehicle with an 11 cm membrane (latex) wing.

Modal analysis of a taught, triangular membrane is given by Sewall et al.[5] The membrane is excited with a shaker, and modal parameters are measured with an eddy current probe. Results are given with membrane pre-tension as a variable for vibration in both air and in a vacuum. Gaspar et al.[6] give similar data for a square membrane, with the eventual goal of progressing research in gossamer spacecraft. Excitation is provided with both an automated impact hammer and a shaker, and measurements are made with a scanning laser Doppler vibrometer (LDV). Modal parameters are reported as a function of membrane pre-stress and excitation locations. Jenkins and Korde[7] provide a comprehensive review of experimental analysis of membrane vibrations, as well as their own research on a circular membrane excited by a small audio speaker located at the membrane's center. A laser vibrometer is used to garner data, with good agreement to analytical results for highly localized mode shapes caused by the small speaker.

Graves et al.[8] present dynamic deformation measurements of a MAVRIC-I semispan wing in a wind tunnel. Measurements from select locations over the wing are made with a high speed videogrammetric system operating at 60 Hz during flutter and limit cycle oscillations. Spectral analysis of the data indicates the prevalent wing modal frequencies. Similar work is presented by Burner et al.[9], with an extension of the videogrammetric technique to in-flight dynamic measurements. Song and Breuer[2] conduct wind tunnel testing of a membrane sheet stretched between two rigid posts at a variety of angles of attack and Reynolds numbers. High speed deformation measurements are made with a two-camera stereo photogrammetry system operating at 1000 Hz. The work locates higher-order membrane vibration modes for certain combinations of α and Reynolds number, suggesting a resonance between the membrane and the flow structures (leading edge vortex shedding).

Albertani et al.[10] perform visual image correlation (VIC) measurements of the static strain state of different configurations of membrane MAV wings in the wind tunnel, confirming the relevance of the pre-strain energy state on the shape and aerodynamic performance of the wings. Ozdoganlar et al.[11] perform experimental modal analysis on microstructures on different specimen configurations and ambient pressures up to 40 mTorr.

This paper takes into consideration the experimental characterization of the dynamics and modal estimates of thin flexible fixed wings during ground vibration testing, as well as the unsteady aeroelastic fluctuations within the steady airflow of a wind tunnel. The effects of the wing membrane pretension upon the modal parameters will also be included. These results support an evaluation of the energy state of flexible wings, and help to determine whether the kinetic energy of the vibrating membrane in a fixed MAV wing (and the kinetic energy converted from elastic energy in a flapping wing) can be converted to useful work. Such a conversion can enhance the potential aerodynamic and control characteristics of artificial flyers, both well-established features in biological fliers.

II. Experimental Setup

A. Test Specimen

Three different benchmark structures were used for repetitions tests: a membrane wing with low pre-tension, a thin beam made of high density foam (50 mm long, 20 mm wide, 3 mm thick), and a taut latex membrane stretched over a rigid aluminum annulus. The wings used in the final tests, illustrated in Figure 2, have a basic structure built around a composite laminate skeleton (the wing root, leading edge, and a thin curved strip that traces the outline of the planform). The carbon fiber skeleton is affixed to a thin, flexible, rubber membrane sheet. The membrane sheet is constrained all along is border, and will thus adaptively inflate during flight for aerodynamic twist. Such a wing structure has been shown to increase both the lift and the longitudinal static stability over its rigid counterpart.

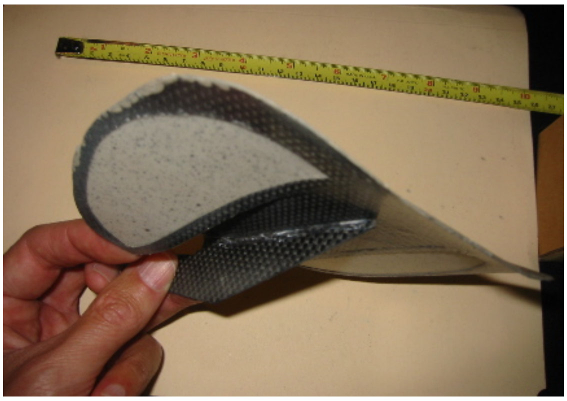

Figure 2. Membrane micro air vehicle wing with a 15 cm span, used for modal and wind tunnel testing.

B. Vibration Measurements

Traditional experimental modal analysis techniques (such as an impact hammer in conjunction with an array of accelerometers) are not suitable for the testing of thin, lightweight membrane structures: non-contact measurement techniques must be applied. For the current work, a scanning laser Doppler vibrometer system (Polytec PSV-400) is used for the structure responses measurements. A laser beam is reflected from the vibrating surface, and the scattered light is detected by the LDV measurement system. The measured shift of the wave (Doppler shift) is proportional to both the object's velocity and the beam's wavelength.

The wing is fixed at the CG location to an electromagnetic shaker (Ling Dynamic Systems V201/3-PA 25E), capable of frequencies up to 13,000 Hz (Figure 3). An interface between the LDV system and the shaker allows for several input control signals: sinusoidal, white noise, chirp and others. For this work, the input force to the structure is selected as the reference signal. This is measured using a piezoelectric load cell (Bruel & Kier 8230) placed between the structure and the shaker, with an estimated sensitivity (a particular concern for the light-weight membrane wings) of 110 mV/N. Furthermore, it is necessary to soft-mount the shaker to a 3 cm thick low-density soft foam pad to mechanically isolate the system, and discourage its own resonance behavior from distorting the measured model parameters.

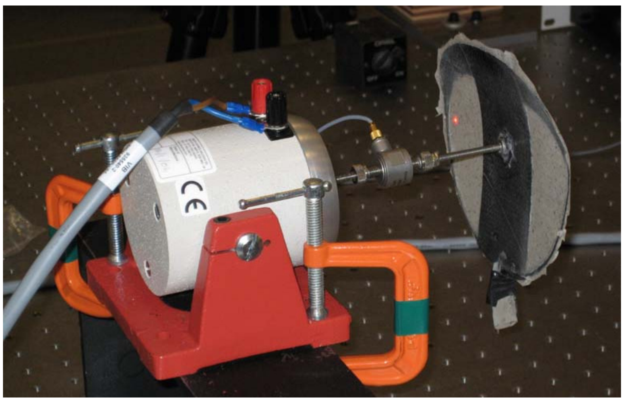

Figure 3. MAV wing mounted to an electromechanical shaker, with a load cell installed in between: a low density foam pad is added for actual testing.

C. Membrane Strain State Measurements

Because the measurements of the strains along a thin membrane must be performed using a non-contact method, a VIC technique is used. The VIC is a non-contacting full-field measurement technique originally developed by researchers at the University of South Carolina[12]. The underlying principle is to calculate the displacement field of a test specimen by tracking the deformation of a subset of a random speckling pattern applied to the surface. Two pre-calibrated cameras digitally acquire this pattern before and after loading, using stereo-triangulation techniques. The VIC system then tries to find a region (in the image of the deformed specimen) that maximizes a normalized cross-correlation function corresponding to a small subset of the reference image (taken when no load is applied to the structure). Such a technique is known as temporal tracking.

Images are captured with two high-speed Phantom v7 CMOS cameras, capable of storing 2900 frames in an in-camera flash-memory buffer. Typical data results obtained from the VIC system consist of geometry of the surface in discrete coordinates (x, y, z) and the corresponding displacements (u, v, w). A post-processing option involves calculating the in-plane strains (ε_{xx}, ε_{yy}, and ε_{xy}). This is done by mapping the displacement field onto an unstructured triangular mesh, and conducting the appropriate numerical differentiation (the complete definition of finite strains is used).

III. Experimental Procedure

The experimental program is divided into two phases: the first to establish general experimental and post-processing analysis criteria; the second using the MAV wing specimen with different levels of membrane pre-tension.

A. Vibration Excitation

Standard excitation methods used for macro structures, such as a shaker directly attached to (or suspended from) the structure or an impact hammer, cannot be applied to MAV components due to their small size and mass. Since one of the key factors for modal analysis is generating frequency response functions (FRFs), an external system is needed to generate the input to the structures. The base excitation using external elements is considered the most promising excitation technique for microstructures[11] and is adopted in this work.

The choice of excitation method is a very relevant factor affecting the quality of the computed FRFs. The application of white noise or a random sinusoidal sweep to the structure does not achieve the required structural excitation, especially in the membrane wings with low or no pre-tension (slack). The burst chirp is considered the best choice for all ranges of membrane pre-tension. Experiments on more rigid structures would most likely be able to make use of the random excitation methods, but the nature of our structures indicate that the burst chirp signal is the best method, with the cleanest results. Typical frequency sweeps range from 5 to 500 or 1,000 Hz. The tests carried out in the wind tunnel do not included artificial structural excitation.

B. Measurement Methods

The scanning LDV can perform an automatic sweep through a grid placed on the target surface image. This image is acquired by a camera mounted on to the laser scanning head. The number of scanning points is varied between 30 and 60. To properly establish phase information between multiple measurements points, a reference signal must be used. Several choices are permitted for this signal, including the input voltage to the shaker, an arbitrarily selected scan point along the surface, or the structure input forces/accelerations. The output signal from the load cell is found to be a suitable choice, representing the true input forces to the structure and having an acceptable signal-to-noise ratio, a feature sometimes unobtainable in micro structures.

For the final tests, the shaker is controlled using a burst chirp signal starting at 3% of the time window and ending at 90% of the window. The burst chirp ranges from 10 Hz to 2 kHz. The rectangular window is applied to all signals, and 5 averages are taken at each data point. The data is sampled with a bandwidth of 1600 Hz and 1600 FFT lines, which yields a spectral resolution of 1 Hz. The data is low-pass filtered at 1500 Hz and sampled at 2.56 kHz. An investigation into the effects of resolution revealed that too precise a resolution will cover peaks with noise, while too course a resolution does not allow one to properly visualize the behavior of the FRF.

C. Wind Tunnel Tests

The facility is an open-loop with a 70 x 70 x 100 cm long open-test section; the maximum free stream velocity is about 10 m/s. The wing is installed in the wind tunnel on a vertical plane, with the suction side facing the VIC cameras as illustrated in Figure 4. The tests are performed at a constant velocity of 9.5 m/s and at three angles of attack: 0º, 15º, and 30º. For the type of membrane wings considered here, $C_{L,max}$ is found[10] to be 1.20 at an angle of attack of 22º; the linear part of the C_L-α curve extends up to 20º with a C_L of 0.85. At an angle of 30º, the wing is completely stalled; at 0º the under-cambered wing has a C_L of 0.10. For every testing condition of α and pre-tension state, images are recorded by the high speed VIC cameras at sampling frequencies of 500 and 1,000 frames/s, and record for a duration of 150 and 300 frames, respectively. The images are processed through the VIC software, using the wind-off conditions as a reference image. Full-field displacements and plain-strains are measured over the entire wing surface for every frame.

Figure 4. MAV wing mounted in the open loop wind tunnel, with twin VIC cameras pointed at the suction side.

D. Post-Processing Methods

After acquisition of vibrations tests, the data is imported into the MEscope VES software package as a structure first, and then as a data block (containing the FRFs at every scan location). At this point a visual inspection of the original spectra (averaged among all of the scan points) associated with the animation of the structure correspondent to the selected frequencies is performed using the Polytec LDV. After a decision as to which frequencies are relevant for the data analysis, an individual or group of peaks is manually selected using the frequency band selector. The alternative of letting the software automatically select the relevant frequencies proved to be impractical; many peaks are selected containing false or spurious modes. Once a group of frequencies peaks are selected, an orthopolynomial fitting method is utilized to determine the modal frequency and damping for that specific peak. When all the frequencies and damping values are determined, the residues are calculated and then the shapes are saved to a shape table.

Repetitions tests on benchmark structures are designed for estimating the confidence interval according to the following equation, valid for a selected percentage probability level:

$$x' = x \pm u_x \ \ (P\%)$$

The uncertainty interval is the value outside the mean that a percentage of all measured values should fall. In the case of an infinite number of measurements, the uncertainty interval should hold universally true for all data within the probability level. In the case of experiments where statistics are finite we introduce the standard deviation:

$$S_x = \left\{ \left(\frac{1}{N-1} \right) \sum_{i=1}^{N} \left(x_i - x \right)^2 \right\}^{1/2}$$

Considering that the standard deviation is only an estimate of the variance, we can modify our initial equation so that we have an uncertainty weighting factor to account for the size of our sample:

$$x' = x \pm t_{v,p} \cdot S_x \ \ (P\%)$$

The t estimate is a function of both the number of measurements taken, and the uncertainty percentage required.

Data from wind tunnel experiments (as opposed to the treatment of the data from the dry vibration tests) are reorganized in the time domain by gathering time histories of the out-of-plane displacements (w) at selected points along the wing surface. The data is then analyzed with a Matlab code, by calculating the FFT and plotting frequency power spectra.

IV. Results

A. Benchmark Tests

The results from repetitions tests in terms of modal frequencies and damping ratios are first plotted by run number. After running an outliers detection scheme, the averages and confidence intervals are estimated, as listed in Table 1.

Table 1. Modal repetition tests for various flexible structures.

Structure	Mode #	Population	Frequency [Hz] Average	Frequency [Hz] 95% Conf. (±)	Damping % Average	Damping % 95% Conf. (±)
Membrane Wing	1	7	27.857	2.611	0.208	0.122
Foam Beam	1	6	70.914	3.160	0.326	0.141
Foam Beam	2	6	393.286	1.194	0.231	0.121
Membrane on Ring	1	16	200.938	0.533	0.042	0.032
Membrane on Ring	2	16	377.250	1.230	0.104	0.030
Membrane on Ring	3	16	394.000	2.201	0.038	0.030

B. Wing Vibration Results

After the basic experimental procedure and data analysis methodology are determined and the confidence interval in the results established, the post processing of the test results is performed. Average spectra (in terms of velocity/force) of the entire wing (carbon fiber and membrane) are depicted in Figure 5 for three cases: high membrane pre-tension (a), low (b) and no pre-tension/slack (c). The spectra of the high and no pre-tension cases are relatively clean in comparison to the low pre-tension. This may be due to the fact that in the first two cases, the membrane modes and carbon modes are comparatively decoupled; in the low pretension case there is no clear dominance of either carbon fiber (bending) or membrane (stretching) strain energy. This also contributes to the mixing of frequency peaks in the low pre-tension spectrum (Figure 5b).

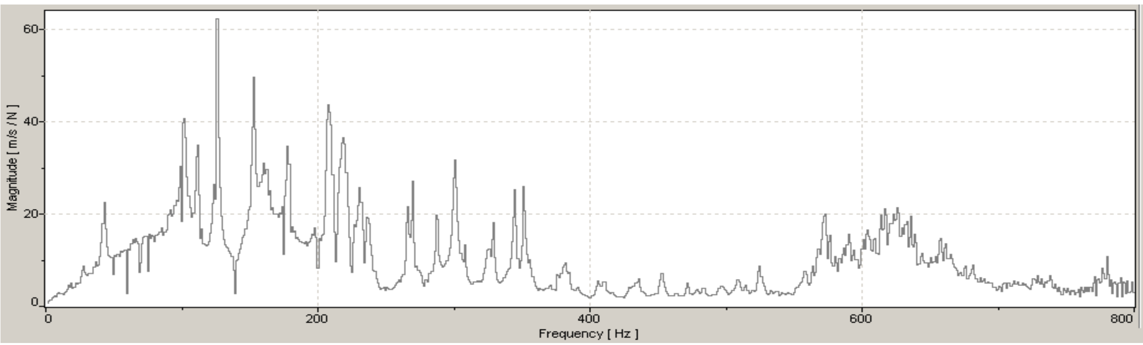

Figure 5a. Average spectra (velocity/force) from LDV testing of membrane wing with high pre-tension.

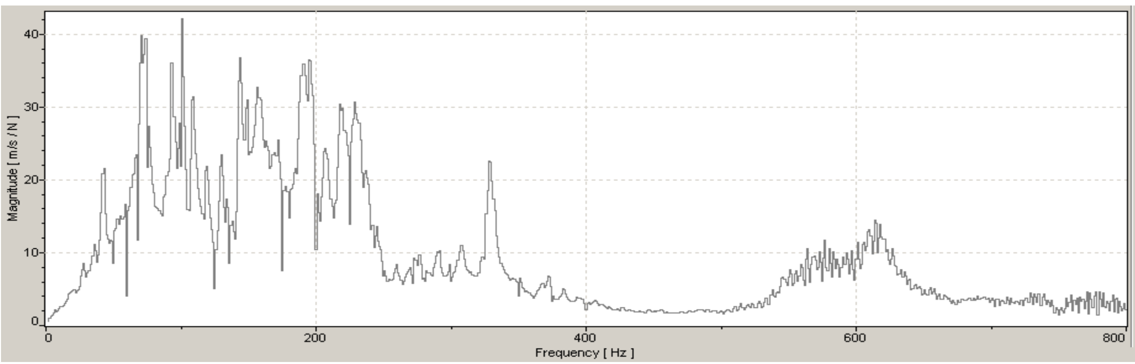

Figure 5b. Average spectra (velocity/force) from LDV testing of membrane wing with low pre-tension.

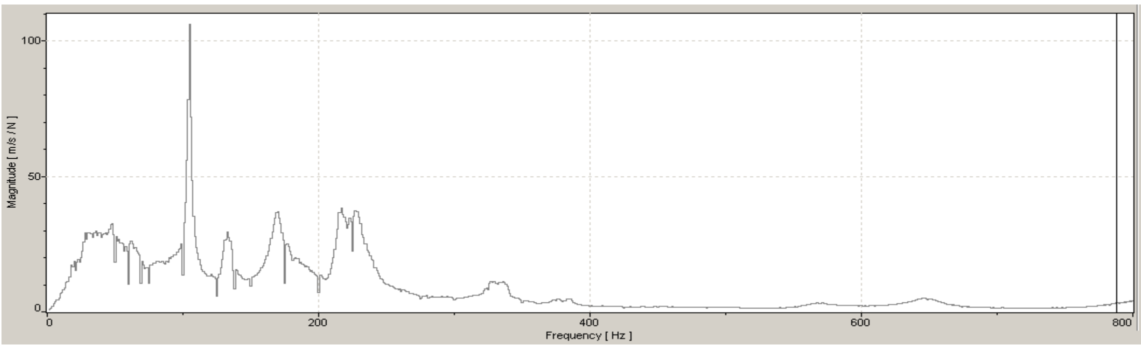

Figure 5c. Average spectra (velocity/force) from LDV testing of membrane wing with no pre-tension.

The membrane pre tension strain state was estimated using the VIC and the results are illustrated in Figure 6 for the three cases of high membrane pretension (a), low (b) and with no pretension (c). Using the modal data obtained by the LDV and the structural dynamics animation features of the Polytec software, the vibrations can be visually separated into membrane and carbon fiber modes for each case. For the carbon fiber structure the first three modes are consistently located at 160, 230 and 330 Hz. A chord-wise mode, characterized by a wing-tail flapping, is always present at a frequency of 100-105 Hz.

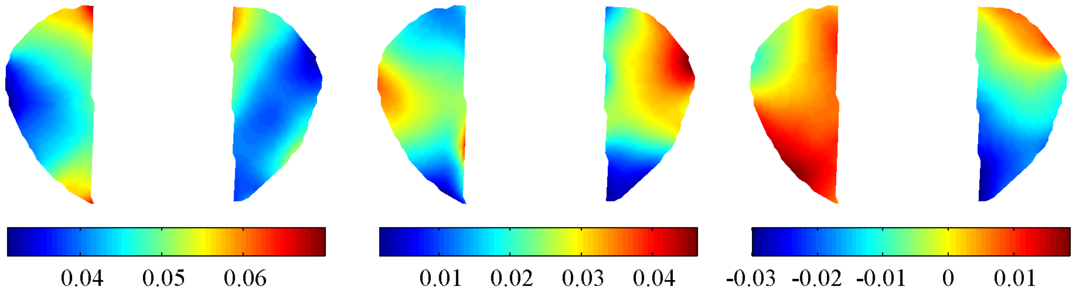

Figure 6a. Chordwise (left), spanwise (center), and shear strains (right) at the high pre-tension level.

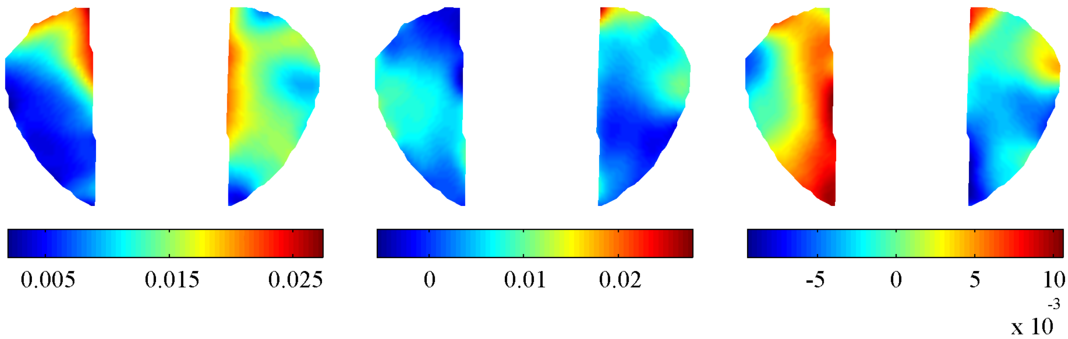

Figure 6b. Chordwise (left), spanwise (center), and shear strains (right) at the low pre-tension level.

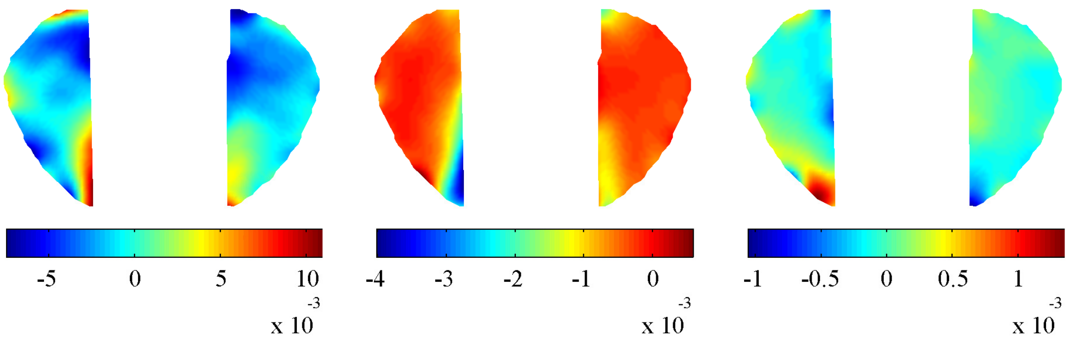

Figure 6c. Chordwise (left), spanwise (center), and shear strains (right) in the slack membrane.

Damping ratios of carbon fiber bending modes (in the case of a high pre-tensioned membrane) display a smooth trend, with values of 0.296% and 0.201% for the first and third mode. In the case of low and no pre-tension, they are very irregular: values are scattered from 0.092% to 0.780%, with a standard deviation up to 0.180. Possible causes for this include viscous damping and coupling between carbon fiber and elastic membrane modes. Future tests in a vacuum chamber will perhaps eliminate the viscous damping effects from the results. The modal parameters have been extracted from the first three modes; results are given in terms of frequencies and damping ratios (Figure 7). The plots contain the cases of high and low membrane pre tension. No clear membrane modes are detected in the slack membrane case; presumably due the overwhelming geometric nonlinearities in this case. Frequencies are shown to increase with mode number, and to contain an irrelevant error bound. The damping ratios decrease with mode number, and the associated error bound is significant for the low pretension case, as expected.

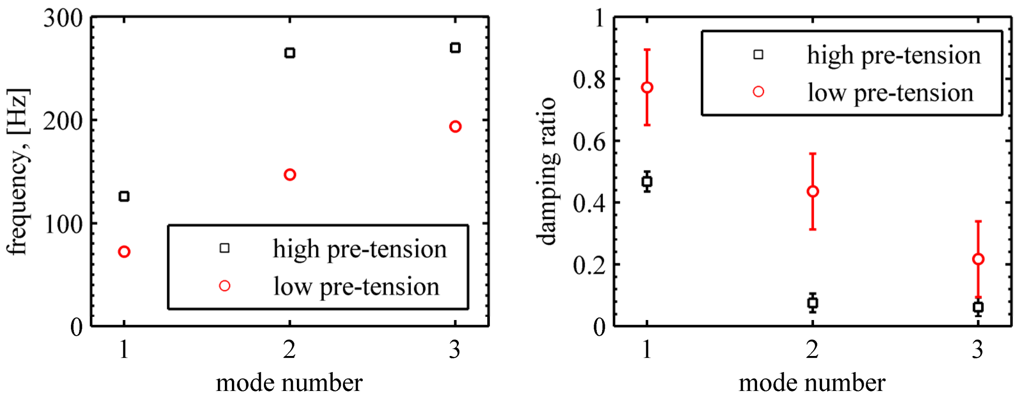

Figure 7. Natural frequencies and damping frequencies for the first three modes.

C. Wind Tunnel Testing Results

A sample of time histories data is depicted in Figure 8, for the three pre-tension states, showing the out-of-plane displacements of three points on the suction side of the wing: x/c=0.32 (black), x/c=0.48 (red) and x/c=0.64 (blue). The span station for all points is at 2y/b=0.71, which lies on the membrane portion of the wing. The angle of attack is fixed at 15º and the free stream velocity is 9.5 m/s. The frame rate (sampling rate) for some cases is 500 frames/s and the total number of frames recorded is 150; with different combinations of pre-tension and α the frame rate is 1,000 with a total number of frames of 300. It can be noted that the displacement without pre strain is higher than the low and high, with less energy at lower frequencies, as expected. Furthermore, the point x/c = 0.48 is very close to the peak of the inflated membrane shape, and hence as the highest displacements. The corresponding power spectra are illustrated in Figure 9, for the same cases and measurements points. The three plots (and all other cases not shown) show some energy in the lower frequencies range between zero and 25 Hz; these are probably due to rigid body motions of the wing on the test stand. For the cases of low and no pre-tension, energy spikes are seen at approximately 100 Hz. This peak is not present in the high pre-tension case or in any case at angles of attack of zero and 30º.

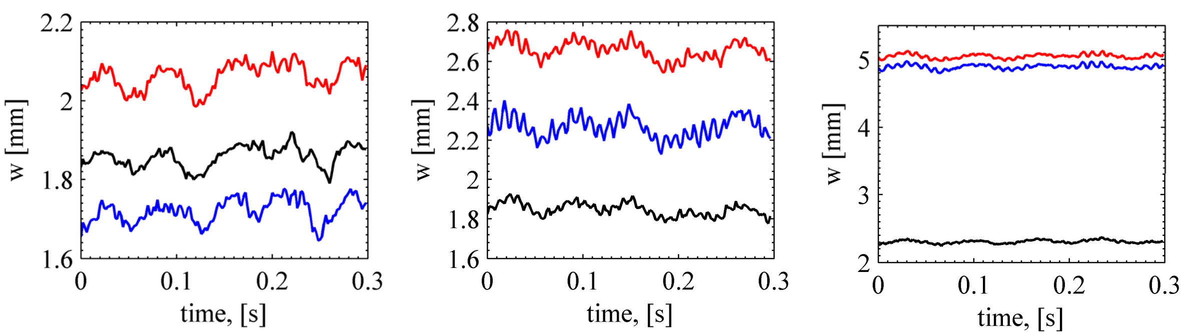

Figure 8. Time history of displacements along the membrane at 15º angle of attack: high (left), low (center), and no pre-tension (right). x/c = 0.32 (black), x/c = 0.48 (red), and x/c = 0.64 (blue) at span station 2y/b = 0.71.

In order to ascertain whether the aforementioned 100 Hz peak could be a membrane aeroelastic effect, frequency spectra are estimated at three points of the wing's carbon fiber root: the leading edge, center, and trailing edge. The data are acquired during the same tests as shown above with the membrane results. The power spectra are illustrated in Figure 10 at three angles of attack: 0º, 15º, and 30º. It is evident from the plots that the energy at lower frequencies relates to the rigid body motions, whereas there is an absence of any appreciable energy at higher frequencies. Since the presence of the 100 Hz peak is evident only on the elastic wing membrane and for certain combinations of α and membrane pre-tension (α = 15^0 with low or no pretension) it is postulated that this energy originates from structure-fluid interactions possibly triggered by vortex shedding (either from the wing tips or the leading edge) or laminar separation bubble effects. Such a resonance at select flight conditions is previously reported by Song and Breuer[2].

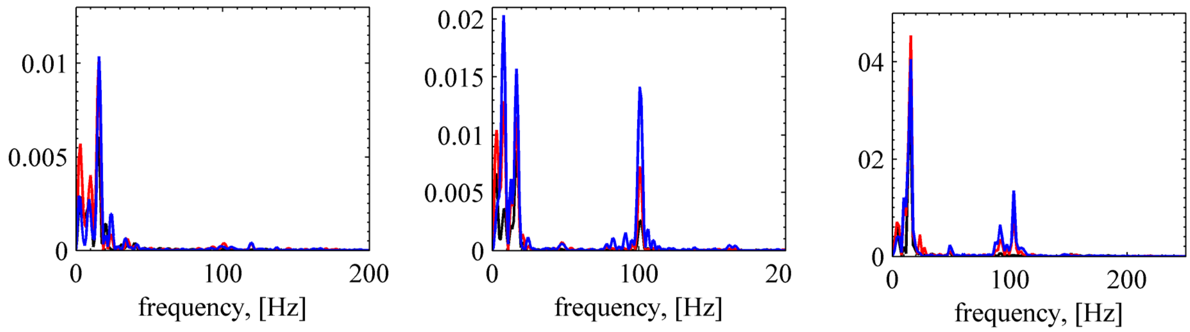

Figure 9. Frequency spectra of displacements along the membrane at 15º angle of attack: high (left), low (center), and no pre-tension (right). x/c = 0.32 (black), x/c = 0.48 (red), and x/c = 0.64 (blue) at span station 2y/b = 0.71.

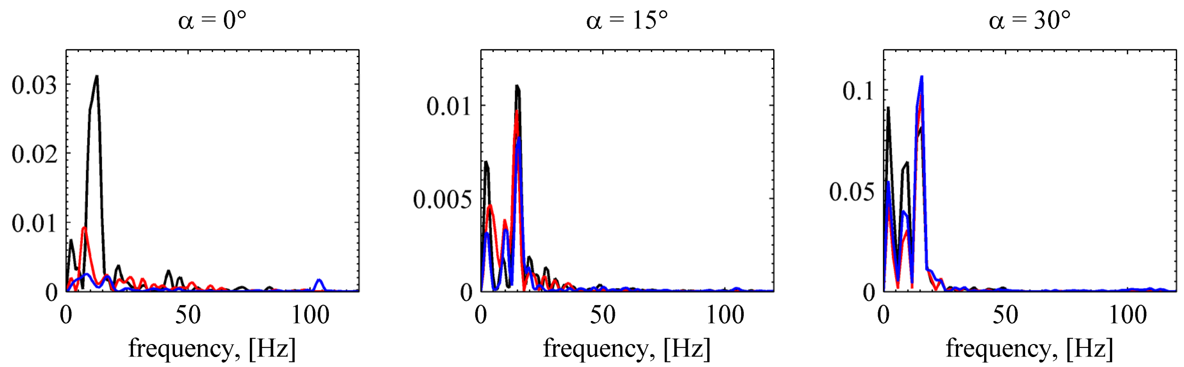

Figure 10. Frequency spectra of displacements along the carbon fiber root, at three angles of attack. x/c = 0 (black), x/c = 0.5 (red), and x/c = 1 (blue) at the wing root.

An overview of the average wing membrane out-of-plane deformations is presented in Figure 11 for the three angles of attack and three pre-tension levels. All the tests are performed at the free stream velocity of 9.5 m/s. Membrane displacement is generally seen to increase with angle of attack for all three levels of tension, even in the post-stall angle of attack regime. Inflation is symmetric for the two semi-wings with high and low pre-tension, but significantly non-symmetric for the slack membrane. This may be a result of bilateral rolling instabilities (wing rock), indicating that the large wing deformations may accelerate the onset of the wing tip vortex (which are very strong for the low aspect ratio considered here) destabilization[13]. Furthermore, that the slack membrane case presents the largest inflation is a clear sign of low frequency, low energy deformations.

V. Conclusions

Bench vibrations tests (dry tests) and naturally induced vibrations measurements in a wind tunnel are performed on 15 cm wingspan flexible membrane wings for MAV applications. The wings are fabricated using a combination of thin bidirectional carbon fiber laminates and a 0.1 mm thin elastic latex membrane as a wing skin. The main objectives of this work are to establish a reliable methodology for modal analysis of light flexible micro structures and apply the procedure to wings with different levels of membrane pre-tension. The results are then used to seek a correlation between the reference strain energy levels and modal characteristics.

The scope of the experimental modal analysis is to determine the modal shapes, natural frequencies and damping of the structures in ambient air, thus including viscous damping effects. Non-contacting measurements (LDV and VIC) and base excitation techniques with an electromagnetic shaker are used.

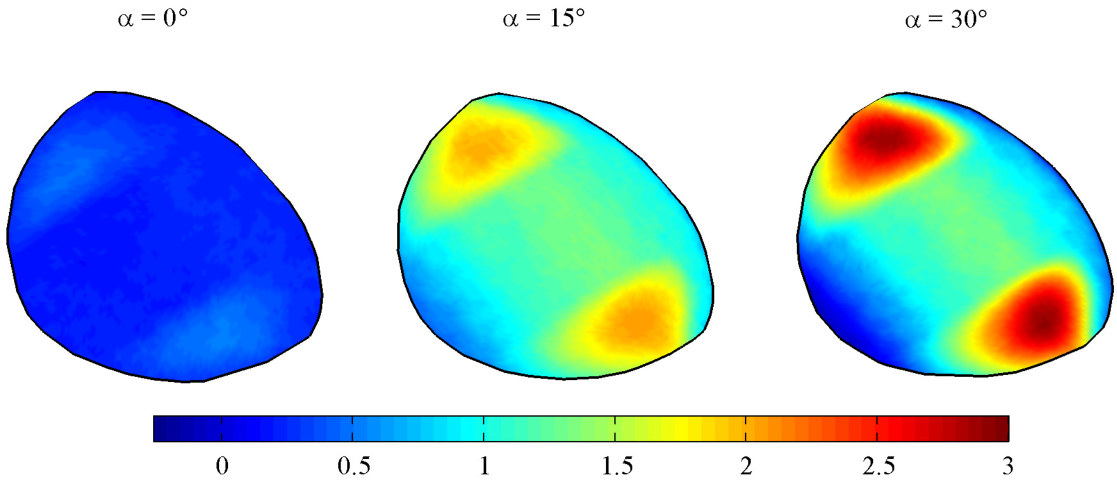

Figure 11a. Time-averaged membrane displacements (mm) of the wing with a high pre-tension.

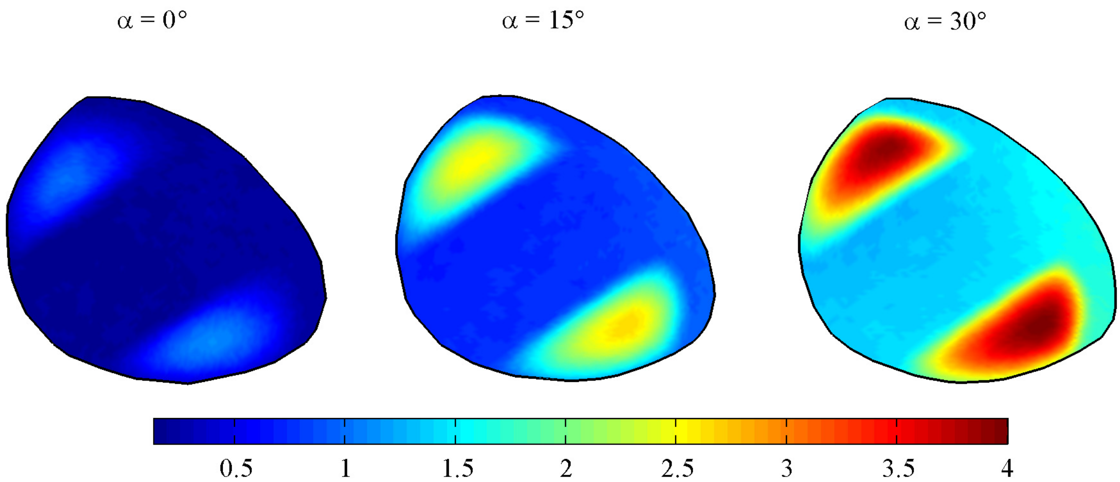

Figure 11b. Time-averaged membrane displacements (mm) of the wing with a low pre-tension.

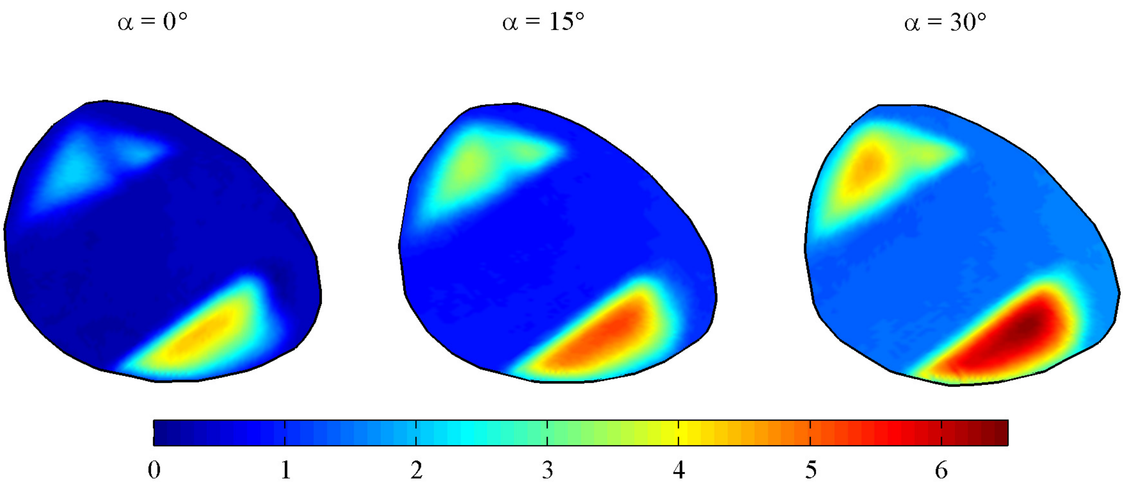

Figure 11c. Time-averaged membrane displacements (mm) of the wing with no pre-tension.

During the dry test experiments a sinusoidal burst chirp type signal is observed to be more effective than a true random signal for structural excitation. Post processing includes Hanning windowing, spectra averaging and curve fitting methods. The experiments in the wind tunnel are conducted at a constant flow velocity and at three angles of attack, including post-stall. The elastic wing's membrane displacements are measured dynamically to obtain time histories and power spectra of the out-of-plane displacements. Results show an acceptable experimental accuracy for the modal parameters. It is possible to decouple the latex membrane modes from the carbon fiber laminate modes in the high and no pre tension cases. The natural frequencies and damping ratios for the elastic membrane are well defined only in the high and low pre tension cases; the first three frequencies modes increase with the pre-tension level while the damping ratio decreases with both the pre-tension level and the mode number, as expected. Wind tunnel tests reveal the presence of an energy spike in the out-of-plane displacements power spectra on the wing membrane at moderate angles of attack for the cases of low and no membrane pre-tension. This spike (approximately 100 Hz) is not a structural vibration mode and is not noticeable on measurements on the carbon fiber wing skeleton. Its presence could thus be induced by unsteady vortex shedding or laminar separation bubble dynamic effects.

Future work will include modal analysis at different ambient pressures, with the specimen in a vacuum chamber. This experiment serves to decouple structural and viscous damping, and will be used in conjunction with the use of different structural wing designs. Wind tunnel tests will be carried out with natural and forced structural excitation including dynamic flow velocity measurements.

Acknowledgements

This work was supported by the Research Institute for Autonomous Precision-Guided Systems under F49620-1-0170 and FA9550-07-1-0236 with Fariba Fahroo as project monitor.

References

1. Raney, D., Slominski, E., "Mechanization and Control Concepts for Biologically Inspired Micro Air Vehicles," *Journal of Aircraft*, Vol. 41, pp. 1257-1265, 2004.
2. Song, A., Breuer, K., "Dynamics of a Compliant Membrane as Related to Mammalian Flight," *45th AIAA Aerospace Sciences Meeting and Exhibit*, Reno, NV, Jan. 8-11, 2007.
3. Lian, Y., Shyy, W., "Laminar-Turbulent Transition of a Low Reynolds Number Rigid or Flexible Airfoil," *AIAA Journal*, Vol. 45, pp. 1501-1513, 2007.
4. Ho, S., Nassef, H., Pornsinsirirakb, N., Tai, Y., Ho, C., "Unsteady Aerodynamics and Flow Control for Flapping Wing Flyers," *Progress in Aerospace Sciences*, Vol. 39, pp. 635-681, 2003.
5. Sewall, J., Miserentino, R., Pappa, R., "Vibration Studies of a Lightweight Three-Sided Membrane Suitable for Space Applications," *NASA Technical Paper*, TP 2095, 1983.
6. Gaspar, J., Solter, M., Pappa, R., "Membrane Vibration Studies Using a Scanning Laser Vibrometer," *NASA Technical Memorandum*, TM 211427, 2002.
7. Jenkins, C., Korde, U., "Membrane Vibration Experiments: An Historical Review and Recent Results," *Journal of Sound and Vibration*, Vol. 295, pp. 602-613, 2006.
8. Graves, S., Bruner, A., Edwards, J., Schuster, D., "Dynamic Deformation Measurements of an Aeroelastic Semispan Model," *Journal of Aircraft*, Vol. 40, pp. 977-984, 2003.
9. Burner, A., Lokos, W., Barrows, D., "Aeroelastic Deformation: Adaptation of Wind Tunnel Measurement Concepts to Full Sale Vehicle Flight Testing," *NASA Technical Memorandum*, TM 213790, 2005.
10. Albertani, R., Stanford, B., Hubner, J., Ifju, P., "Aerodynamic Characterization and Deformation of a Flexible Wing Micro Air Vehicle," *Experimental Mechanics*, DOI: 10.1007/s11340-006-9025-5.
11. Ozdoganlar,O., Hansche, B., Carne, T., "Experimental Modal Analysis for Microelectromechanical Systems," *Experimental Mechanics*, Vol. 45, pp. 498-506, 2006.
12. Sutton, M., Cheng, M., Peters, W., Chao, Y., McNeill, S., "Application of an Optimized Digital Image Correlation Method to Planar Analysis," *Image and Vision Computing*, Vol. 4, pp. 143-151, 1986.
13. Jian, T., Ke-Qin, Z., "Numerical and Experimental Study of Flow Structure of Low-Aspect-Ratio Wing," *Journal of Aircraft*, Vol. 41, pp. 1196-1201, 2004.